Dalton Transactions

Synthesis, Structure, and Electrochemical Properties of $[LNi(R_f)(C_4F_8)]^-$ and $[LNi(R_f)3]^-$ Complexes

Journal:	*Dalton Transactions*
Manuscript ID	DT-ART-02-2022-000511.R1
Article Type:	Paper
Date Submitted by the Author:	08-Mar-2022
Complete List of Authors:	Shreiber, Scott; Lehigh University, Department of Chemistry Amin, Fatema; Lehigh University, Department of Chemistry Schäfer, Sascha; University of Cologne, Chemistry Cramer, Roger; University of Hawaii, Department of Chemistry Klein, Axel; University of Cologne, Chemistry Vicic, David; Lehigh University, Department of Chemistry

Synthesis, Structure, and Electrochemical Properties of $[LNi(R_f)(C_4F_8)]^-$ and $[LNi(R_f)_3]^-$ Complexes

Scott T. Shreiber,[#a] Fatema Amin,[#a] Sascha A. Schäfer,[b] Roger E. Cramer,[c] Axel Klein [b*] and David A. Vicic[a*]

[a] Department of Chemistry, Lehigh University, 6 E Packer Ave., Bethlehem, PA 18015, USA. E-mail: sts217@lehigh.edu; ORCID: 0000-0002-4224-7461 (S.T.S); E-mail: fab319@lehigh.edu; ORCID: 0000-0002-8420-1912 (F.A.).
[b] University of Cologne, Faculty of Mathematics and Natural Sciences, Department of Chemistry, Institute for Inorganic Chemistry, Greinstrasse 6, 50939 Koeln, Germany. E-mail: sascha.schaefer@uni-koeln.de; ORCID: 0000-0001-6035-1281 (S.A.S.).
[c] Department of Chemistry, University of Hawaii, 2545 McCarthy Mall, Honolulu, HI, 96822, USA. E-mail: rcramer@hawaii.edu ORCID: 0000-0002-3934-3401 (R.E.C.).

* Corresponding authors: E-mail: axel.klein@uni-koeln.de, ORCID: 0000-0003-0093-9619; Tel.: +49-221-470-4006 (A.K.). E-mail: vicic@lehigh.edu; fax, 1-610-758-6536, ORCID: 0000-0002-4990-0355 (D.A.V.)

Dalton Trans. received

Abstract: The new anionic nickelate complexes $[(MeCN)Ni(C_4F_8)(CF_3)]^-$, $[(MeCN)Ni(C_4F_8)(C_2F_5)]^-$, $[(IMes)Ni(C_4F_8)(CF_3)]^-$, $[(IMes)Ni(CF_3)_3]^-$ (IMes = 1,3-bis(2,4,6-trimethylphenyl)imidazol-2-ylidene), and $[(F\text{-NHC})Ni(R_F)_3]^-$ (*F*-NHC = 1,3-bis(2,4-F_2Ph), 2,4,6-F_3Ph- or 3,4,5-F_3Ph)imidazol-2-ylidene; R_f = CF_3 or C_2F_5) were synthesized and structurally characterized. The electrochemical properties of all new compounds were revealed by cyclic voltammetry studies and compared to the known CF_3 analogue $[(MeCN)Ni(CF_3)_3]^-$. The IMes-coordinated complexes exhibited initial oxidation events that were well-separated from a second oxidation process in the cyclic voltammograms. The complexes containing F-substituted NHC ligands $[(F\text{-NHC})Ni(CF_3)_3]^-$ are structurally quite similar to the IMes derivative and reveal also two separated oxidation waves in their cyclic voltammograms. The absolute potentials as well as the separation between the two waves vary with the substitution pattern, suggesting that the NHC ligand environment (NHC = *N*-heterocyclic carbene) is an interesting platform for the development of new redox-triggered reactions that release trifluoromethyl and perfluoroalkyl radicals upon oxidation.

Keywords: Nickel, fluoroalkylation, NHC ligands, electrochemistry

Introduction

Nickel is a promising platform for the development of new synthetic methodologies involving fluoroalkyl groups. Two fundamentally different ways for Ni to mediate $C–C_{fluoroalkyl}$ bond forming reactions are shown in Eq. 1 and 2.

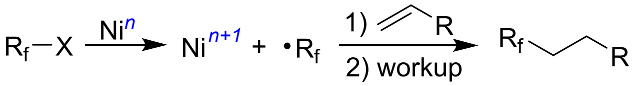

(1)

catalysis observed for R_f = CF_3 and fluoroalkyl

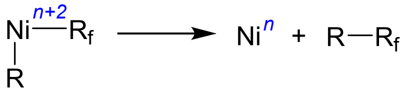

(2)

catalysis observed for R_f = fluoroalkyl only

It is known that low valent Ni can react with perfluoroalkyl electrophiles to generate perfluoroalkyl radicals (Eq. 1), which can in turn undergo additions to a variety of organic substrates like alkenes. Catalytic fluoroalkylations of this type have been demonstrated with Ni for both the trifluoromethyl[1-4] and fluoroalkyl[4-7] groups. Another mechanistic pathway for C–$C_{\text{fluoroalkyl}}$ bond forming reactions involves a discrete reductive elimination event as described in Eq. 2. Catalysis involving putative reductive eliminations at Ni are only known for fluoroalkyl[8-11] and difluoromethyl,[12-14] but not for trifluoromethyl. Stoichiometric reductive eliminations involving trifluoromethyl groups have been demonstrated for high-valent [Ni(R)(CF_3)] complexes experimentally[15-19] and computationally,[20] but to our knowledge these elimination reactions have not been included in catalytic transformations at Ni.

Our group has been developing the use of solvent complexes of Ni as reagents for the trifluoromethylation of organic electrophiles, and we have recently shown that $[(MeCN)Ni(R_f)_3]^-$ (R_f = CF_3, C_2F_5) reacts with aryl iodonium, alkynyl iodonium, and diazonium salts to afford fluoroalkylated arenes in moderate to good yields.[16,21] Further studies have shown that the homoleptic $[Ni(CF_3)_4]^{2-}$ can catalyze C–H bond trifluoromethylations of electron-rich (hetero)arenes in up to 99% yield (Scheme 1).[21]

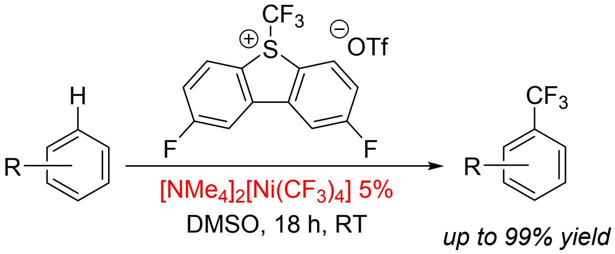

Scheme 1. Trifluoromethylation using $[NMe_4]_2[Ni(CF_3)_4]$ as catalyst. Adopted from ref. 20.

One modification to this system that we sought to explore was the replacement of two of the spectator trifluoromethyl groups with a chelating C_4F_8 ligand. The motivation behind this change is that we[22,23] and others[24] have demonstrated that high-valent [Ni(C_4F_8)] complexes are oxidatively more stable than [Ni$(CF_3)_2$] derivatives and do not readily suffer from reductive homolyses reactions that often occurs with the [Ni$(CF_3)_2$] counterparts. The C_4F_8 ligand also appears to be less sensitive to α-fluoride abstraction processes with trace amounts of Lewis acids relative to trifluoromethyl derivatives, which in turn renders the C_4F_8 complexes more stable towards adventitious water.[25,26] Only when very strong Lewis acids are used, such as BCl_3, BF_3, and Me_3SiOTf have fluoride abstractions at the C_4F_8-containing metallacycle been reported.[27,28] Well-defined Ni(III) and Ni(IV) species with the C_4F_8 ligand have now been reported to be robust enough to be isolated and stored on the benchtop.[23,24] Given the aforementioned qualities of the C_4F_8 ligand, we targeted the synthesis of $[(L)Ni(R_f)(C_4F_8)]^-$ in order to characterize their chemical and electrochemical properties with their non-chelating fluoroalkyl counterparts.

Results and Discussion

Syntheses and structures

Complexes of the type $[(MeCN)Ni(C_4F_8)(R_f)]^-$ (**2** and **3** (Eq. 3)) with $[NMe_4]^+$ counter ions were successfully prepared by reacting the known[29] $[(MeCN)_2Ni(C_4F_8)]$ (**1**) with $Me_3Si–R_f$ ($R_f = CF_3$ or C_2F_5) in the presence of AgF and NMe_4Cl (for details, see Experimental Section). Complex **2** displays a diagnostic ^{19}F NMR signal for the $Ni–CF_3$ resonance at $\delta = –31.4$ (quintet, $J = 3.5$ Hz) in CD_3CN solvent (Fig. S14 in the Electronic Supporting Information, ESI), whereas the CF_3 resonance of the perfluoroethyl ligand in complex **3** occurred at $\delta = –82.5$ (t, $J = 3.8$ Hz, 3F) (Fig. S16, ESI). The structures of complexes **2** and **3** were further confirmed by X-ray crystallography (crystal structures in Figs. S1 and S2), and ORTEP diagrams are provided in Fig. 1. Both complexes adopt a square-planar geometry in the solid state, with the C–Ni–C bond angles of the perfluoro-metallacyclopentane units slightly smaller than any other angles in the square planes involving the Ni centers. The MeCN ligands in **2** and **3** are clearly less *trans* influencing than the fluoroalkyl ligands, and the CF_2 groups that are spatially opposing the acetonitriles in both structures bear the shortest Ni–C bonds.

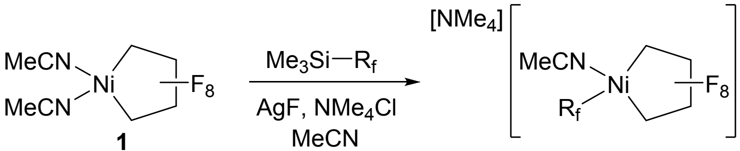

(3)

1

2, $R_f = CF_3$ 72%
3, $R_f = C_2F_5$ 75 %

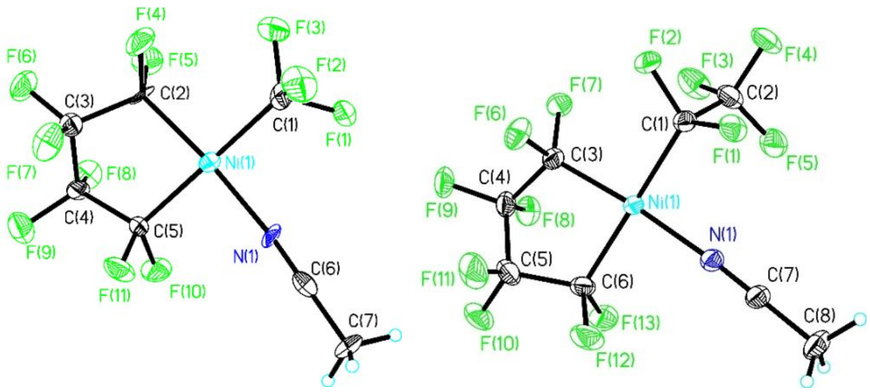

Fig. 1 ORTEP diagram of **2** (left) and **3** (right). Ellipsoids shown at the 40% level. **2**: Counter-ions and co-crystallized solvents are omitted for clarity. Selected bond lengths (Å) for 2: Ni1–N1 1.895(3); Ni1–C2 1.897(4); Ni1–C5 1.934(4); Ni1–C1 1.957(4); N1–C6 1.137(5). Selected bond angles (°) for **2**: N1–Ni1–C2 170.67(15); N1–Ni1–C5 89.31(15); C2–Ni1–C5 86.91(16); N1–Ni1–C1 92.09(14); C2–Ni1–C1 92.38(15); C5–Ni1–C1 175.10(17); C6–N1–Ni1 173.3(4). Selected bond lengths (Å) for **3**: Ni1–N1 1.8938(15); Ni1–C3 1.8967(18); Ni1–C6 1.9330(19); Ni1–C1 1.9556(18); N1–C7 1.136(2). Selected bond angles (°) for **3**: N1–Ni1–C3 174.49(7); N1–Ni1–C6 88.14(7); C3–Ni1–C6 86.69(8); N1–Ni1–C1 91.65(7); C3–Ni1–C1 93.64(8); C6–Ni1–C1 176.16(8); C7–N1–Ni1 176.16(8).

The effect of ligands on the electronic properties of the nickelates was then explored by reacting **2** with *N*-heterocyclic carbenes. Reaction of **2** with IMes (1,3-bis(2,4,6-trimethylphenyl)imidazol-2-ylidene) in MeCN solution led to the formation of the ligated $[(IMes)Ni(CF_3)(C_4F_8)]^-$ (**4**), isolated as $[NMe_4]^+$ salt in 69% yield (Eq. 4). The ^{19}F NMR spectrum of **4** in CD_3CN reveals the diagnostic $Ni–CF_3$ resonance at $\delta = –$

23.2 (br s, 3F) (Fig. S18). A preliminary X-ray structure confirming the connectivity of compound **4** was also obtained and is provided in Fig. S3.

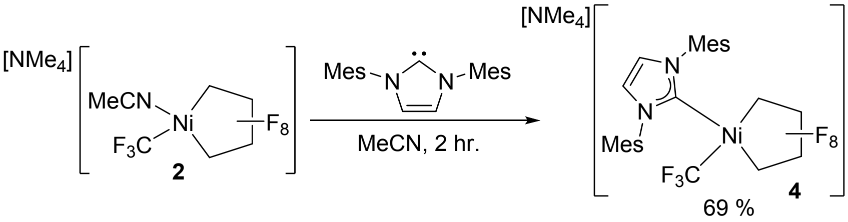

(4)

For comparison with $[(IMes)Ni(CF_3)(C_4F_8)]^-$, we have also prepared the non-C_4F_8 analogue $[(IMes)Ni(CF_3)_3]^-$ (**6**). Reaction of the solvent complex **5** with IMes in MeCN solvent cleanly led to the formation of **6** in 66% yield (Eq. 5) as $[NMe_4]^+$ salt. The ^{19}F NMR of **6** displayed a reversal in the relative positions of the different CF_3 groups with respect to **5**, with the equivalent *trans* CF_3 groups resonating at higher frequencies (δ –22.9 (q, *J* = 5.3 Hz, 6F) and –26.8 (sept, *J* = 5.3 Hz, 3F) (Fig. S20). Complex **6** was also structurally characterized (Fig. 2 and Fig. S4). The X-ray data show that the strongly donating NHC ligand of **6** exhibits much more of a *trans* effect than the MeCN ligands in complexes **2** and **3**, as the CF_3 group that is *trans* to the NHC bears a Ni–C distance that is more on par with the two symmetrically equivalent CF_3 groups that are *trans* to each other.

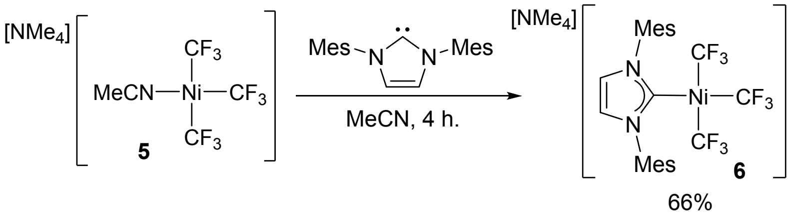

(5)

The complex $[Ni(IMes)(CF_3)_3]^-$ was also crystallized with $[PPh_4]^+$ cations and a co-crystallized MeCN molecule with a very similar crystal and molecular structure (Figs. S5 and S6 ESI).

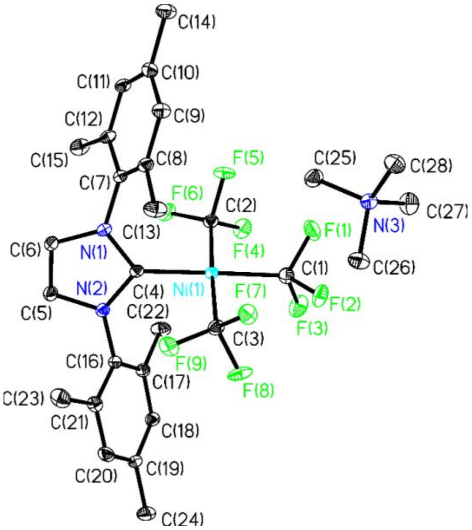

Fig. 2. ORTEP diagram of **6.** Ellipsoids shown at the 40% level. Selected bond lengths (Å): Ni1–C4 1.923(5); Ni1–C1 1.939(5); Ni1–C2 1.949(5); Ni–C3 1.959(5); N1–C4 1.369(6); N2–C4 1.378(6). Selected bond angles (°) for **6**: C4–Ni1–C1 176.6(2); C4–Ni1–C2 90.6(2); C1–Ni1–C2 87.7(2); C4–Ni1–C3 91.8(2); C1–Ni1–C3 90.0(2); C2–Ni1–C3 177.5(2); N1–C4–N2 102.9(4).

In a very similar fashion, we reacted F-substituted NHC ligands (Eq. 6) with compound **5** which led to the complexes [(*F*-NHC)Ni(R_f)$_3$]$^-$ (*F*-NHC = 1,3-bis(2,4-F_2Ph)$_2$- (**7**), 2,4,6-F_3Ph- (**8**), or 3,4,5-F_3Ph)imidazol-2-ylidene (**9**); R_f = CF_3 or C_2F_5) which crystallized as [NMe_4]$^+$ salts.

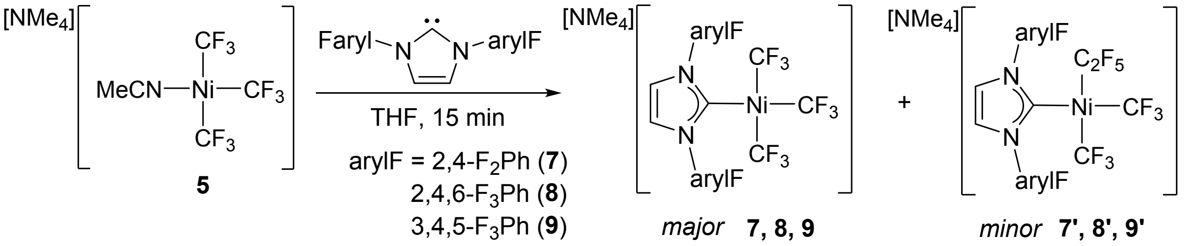

(6)

Close examination of the ^1H and ^{19}F NMR spectra for **7–9** revealed the presence of a minor species for each derivative where one of the CF_3 ligands had been converted to C_2F_5 (Figs. S21 to S23). It has long been known that conditions leading to the preparation of metal-CF_3 complexes can also generate metal-C_2F_5 byproducts, presumably through F–M=CF_2 intermediates.[30-32] The conditions to prepare **7–9** were slightly different than those used to prepare **2–6**, which likely contributed to the greater formation of perfluoroethyl substituents in **7–9**. Crystallization could not separate **7-9** from their respective perfluoroethyl decomposition products **7′–9′** in bulk syntheses. X-ray diffraction analysis of **9** (Fig. 3), for example, showed split occupancies for the CF_3 and C_2F_5 ligands the same positions (crystal structure in Figs. S9 and S10).

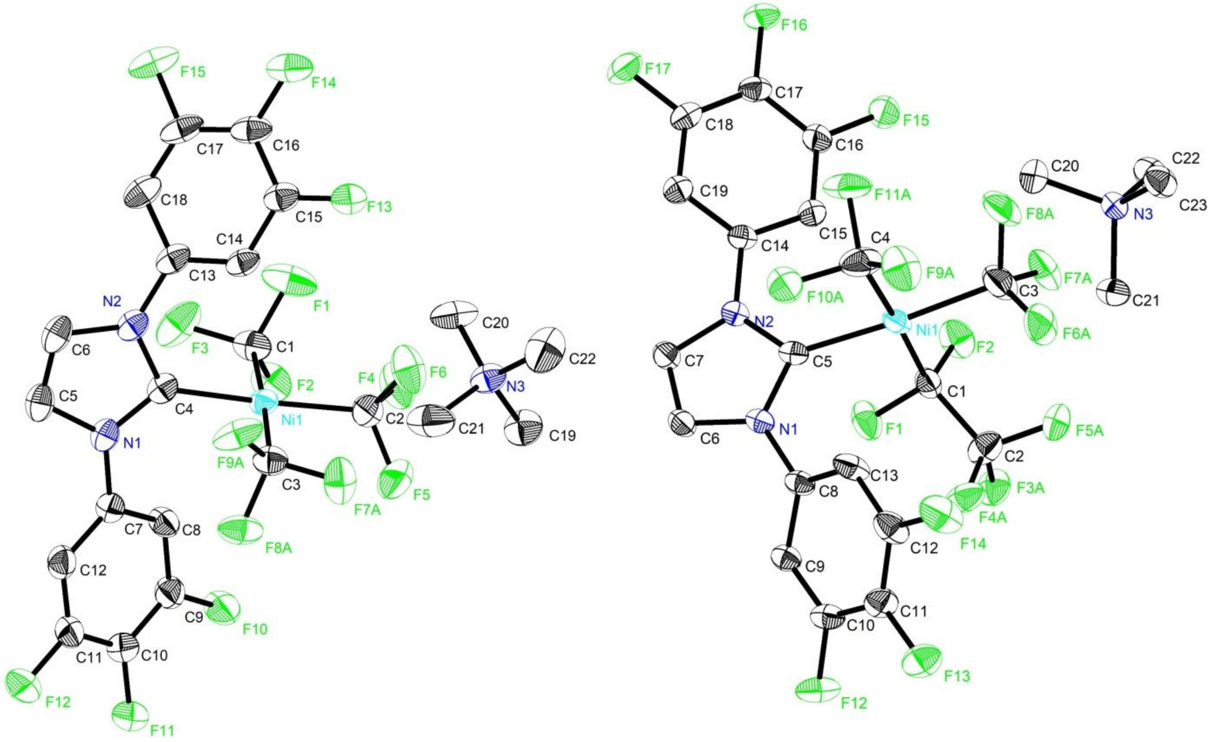

Fig. 3 ORTEP diagrams of separately crystallized **9** and **9′**. Ellipsoids shown at the 40% level. Hydrogen atoms are omitted for clarity. Additionally for **9′** two equivalents of co-crystallized THF are omitted for clarity. Rotational disorders at C3 (**9**), C2 (**9′**) and C3 (**9′**), as well as a –CF_3/–C_2F_5 disorder on C4 (**9′**) are

omitted as well. Selected bond lengths in **9** (Å): Ni1–C1 1.9551(56); Ni1–C2 1.9125(52); Ni1–C3 1.9314(49); Ni1–C4 1.8910(47). Selected bond angles for **9** (°): C1–Ni1–C2 90.986(236); C1–Ni1–C3 176.862(214); C1–Ni1–C4 89.325(212); C2–Ni1–C3 91.291(228); C2–N1–C4 176.574(216); C3–Ni1–C4 88.530(207). Selected bond lengths in **9′** (Å): Ni1–C1 1.9689(27); Ni1–C3 1.9276(39); Ni1–C4 1.9572(38); Ni1–C5 1.8926(26). Selected bond angles for **9′** (°): C1–N1–C3 92.71(13); C1–Ni1–C4 177.12(12); C1–Ni1–C5 89.51(10); C3–Ni1–C4 90.17(15); C3–Ni1–C5 176.43(12); C4–Ni1–C5 87.60(12).

Electrochemical studies

The electrochemical properties of compounds **1** and **5** and of all new complexes were investigated by cyclic voltammetry (CV). Fig. 4 shows representative plots (the remaining CVs can be found in Figs. S24–S27), and Table 1 summarizes the electrochemical data.

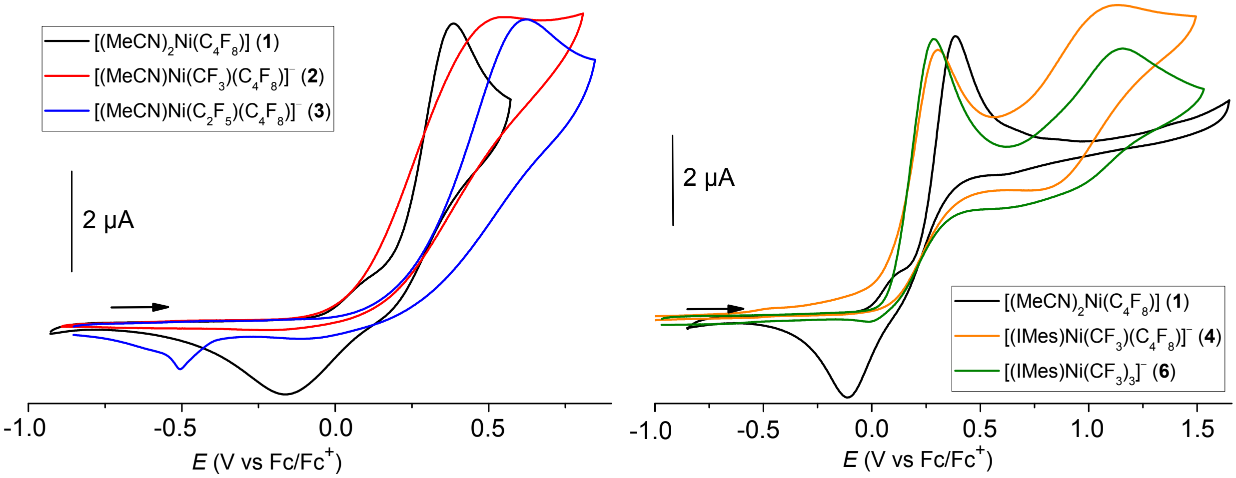

Fig. 4 Cyclic voltammograms of **1** (black), **2** (red), and **3** (blue) (to the left) and **1** (black), **4** (orange), and **6** (green) (to the right) in MeCN/*n*-Bu$_4$NPF$_6$.

Table 1. Selected electrochemical data of Ni complexes.[a]

compound	**Ox 1**	**Ox 2**	
	E_{pa}	E_{pa}	ΔE
[(MeCN)$_2$Ni(C$_4$F$_8$)] **1**	0.39 [b]		
[(MeCN)$_2$Ni(CF$_3$)$_2$]	0.76		
[(MeCN)Ni(CF$_3$)$_3$]$^-$ **5**	0.38	0.51	0.13
[Ni(CF$_3$)$_4$]$^{2-}$	0.10 [c]	0.50 [c]	0.40
[(MeCN)Ni(C$_4$F$_8$)(CF$_3$)]$^-$ **2**	0.53		
[(MeCN)Ni(C$_4$F$_8$)(C$_2$F$_5$)]$^-$ **3**	0.63		
[(IMes)Ni(CF$_3$)(C$_4$F$_8$)]$^-$ **4**	0.30	1.13	0.83
[(IMes)Ni(CF$_3$)$_3$]$^-$ **6** [d]	0.28	1.14	0.86
[(*F*-NHC)Ni(CF$_3$)$_3$]$^-$ (2,4-F$_2$Ph) **7**	0.47	0.84	0.37
[(*F*-NHC)Ni(CF$_3$)$_3$]$^-$ (2,4,6-F$_3$Ph) **8**	0.39 [b]	1.09	0.70
[(*F*-NHC)Ni(CF$_3$)$_3$]$^-$ (3,4,5-F$_3$Ph) **9**	0.54	1.25	0.71

[a] Electrochemical potentials (V) measured in *n*-Bu$_4$PF$_6$/MeCN at 298 K, scan rate 100 mV/s with an accuracy of ±0.003 V, vs. the ferrocene/ferrocenium (Fc/Fc$^+$) couple; E_{pa} for irreversible oxidation waves. [b] Partially reversible. [c] From ref. 16. [d] Additional irreversible reduction waves at –2.25 and –2.91 which were not observed for the other compounds (Figs. S25 and S26).

Oxidation of **1** is partially reversible, with a peak potential for the oxidation at +0.39 V vs. the ferrocene/ferrocenium (Fc/Fc$^{+)}$ couple (Fig. 4, black line). The oxidation of **1** occurs at a peak potential much less positive than for the related trifluoromethyl derivative [(MeCN)$_2$Ni(CF$_3$)$_2$], which occurs at +0.76 V,[16] indicating that the trifluoromethyl group is more globally stabilizing in this family of complexes. Similar trends in the redox properties of C_4F_8 vs CF_3 complexes of Ni bipyridine[22,33] and terpyridine[23,34] have been reported. The large differences in these baseline values for the C_4F_8 and CF_3 parent Ni complexes appear to play a role in the degree to which anation affects the oxidation potentials of derivatives bearing an additional trifluoromethyl or perfluoroalkyl group. For instance, we show here that the oxidation peak potentials of the C_4F_8-bearing anionic complexes **2** and **3** display only minor differences (+0.53 V and +0.63 V, Fig. 4, red and blue lines, respectively), and that anation confers a slight stabilization relative to the parent [(MeCN)$_2$Ni(C$_4$F$_8$)] complex with respect to oxidation. Addition of formally anionic trifluoromethyl ligands to the parent [(MeCN)$_2$Ni(CF$_3$)$_2$] complex, however, is known to result in complexes that are easier to oxidize. For instance, [(MeCN)Ni(CF$_3$)$_3$]$^-$ and [Ni(CF$_3$)$_4$]$^{2-}$ display peak potentials at +0.38 and +0.10 V, respectively, far removed from the potential needed to oxidize [(MeCN)$_2$Ni(CF$_3$)$_2$] (+0.76 V).[16] The complete irreversibility of the waves for **2** and **3** in Fig. 4 (left) is believed to be a result of fast reductive homolysis of CF_3 and C_2F_5 radicals from electrogenerated Ni(III) intermediates.[16,20]

The IMes complex **4** has a first peak potential at +0.30 V vs. the Fc/Fc$^+$ couple, which is 0.23 V easier to oxidize than the solvent complex [(MeCN)Ni(C$_4$F$_8$)(CF$_3$)]$^-$ (**2**). Thus, the greater electron donating ability of the NHC ligand relative to the MeCN is readily observable for these nickelate species by cyclic voltammetry. More interesting, however, is the result that complex **4** exhibits a well-formed second oxidation peak at +1.13 V, whereas complexes **1–3** do not (Fig. 4 (right), orange line vs. black). We suggest that upon electrooxidation of **4**, the resulting [(IMes)Ni^{III}(C$_4$F$_8$)(CF$_3$)] eliminates a CF_3 radical to afford the three-coordinate[28] and charge neutral [(IMes)Ni^{II}(C$_4$F$_8$)], and the oxidation wave at +1.13 V corresponds to the oxidation of the [(IMes)Ni^{II}(C$_4$F$_8$)]. We speculate that the differences in coordination numbers between [(IMes)Ni(C$_4$F$_8$)] and [(IMes)Ni(CF$_3$)(C$_4$F$_8$)]$^-$ contributes to the separation of the oxidation peaks.

The cyclic voltammogram of **6** is very similar to the one of **4** (Fig. 4 right) and very similar potentials were recorded (Table 1). Comparison of the two related complexes [(MeCN)Ni(CF$_3$)$_3$]$^-$ (**5**) and [(IMes)Ni(CF$_3$)$_3$]$^-$ reveals that the IMes ligand facilitates the oxidation compared with the MeCN ligand, which is probably due to the superior σ-donation power of the NHC ligand. The known **5** displays also two closely spaced oxidation peaks (Fig. S25),[16] but the separation of the second oxidation peak for **4** and **6** is much larger and therefore, the observed peak separation is inherently related to the NHC ligand, and not the nature of the perfluoroalkyl substituents.

This is confirmed by the behavior of the three complexes [(*F*-NHC)Ni(CF$_3$)$_3$]$^-$ (**7–9**) (Figs. S26 and S27) which show also two separated oxidation waves. The first oxidation potentials increase along the series 2,4,6-F$_3$Ph (**8**) < 2,4-F$_2$Ph (**7**) < 3,4,5-F$_3$Ph (**9**) which goes along with a partially reversible behavior for **8**, while **7** and **9** show completely irreversible waves. Interestingly, the *F*-NHC complex **8** and the MeCN derivative **5** exhibit very similar first oxidation potentials. The separation between first and second oxidation is slightly smaller for the *F*-NHC complexes **8** and **9** compared with the IMes derivatives **4** and **6**. The difluorophenyl complex **7** shows a relatively small separation, the specific substitution pattern of this F-NHC ligand must be the reason for this.

This ability to significantly separate the two oxidation events by the addition of ancillary ligands like NHCs bodes well for preventing over-oxidation pathways during the optimization of new electrochemical methods that rely on one electron oxidations of [LNi(R$_f$)$_3$]$^-$ derivatives in order to release R$_f$ radicals.

Preliminary catalytic studies

Because the oxidation of complex **2** is within the window of common oxidants,[35] we examined if **2** could also serve as a catalyst for the C–H bond trifluoromethylation of arenes as described in Eq. 7. Indeed, reaction of 1,3,5-trimethoxybenzene with Umemoto Reagent II in DMSO solvent with 5 mol% **2**, yielded trifluoromethylated product in 83% yield (Eq. 7). For comparison, the non-chelated $[(MeCN)Ni(CF_3)_3]^-$ gave a 78% yield of product in a prior report, and the dianionic $[Ni(CF_3)_4]^{2-}$ afforded product in 96% yield.[20]

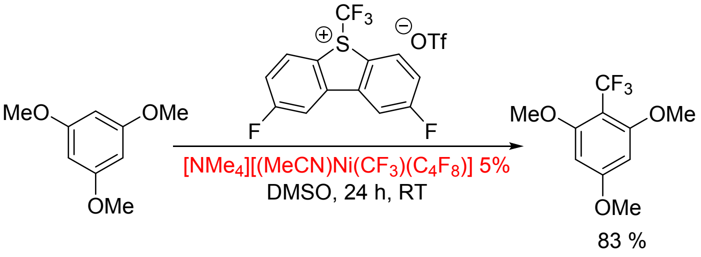

(7)

Conclusions

The modularity of the $[L_2Ni(R_f)_2]$ and $[LNi(R_f)_3]^-$ system was exploited in order to reveal the electrochemical properties of derivatives that bear different perfluoroalkyl substituents as well as different dative ligands MeCN or NHC. Significant differences in oxidation potentials were observed for the charge neutral $[(MeCN)_2Ni(C_4F_8)]$ versus $[(MeCN)_2Ni(CF_3)_2]$, with the former being much easier to oxidize. Anation to afford $[(MeCN)Ni(C_4F_8)(R_f)]^-$ (R_f = CF_3 or C_2F_5) and $[(MeCN)Ni(CF_3)_3]^-$ however, showed somewhat of a leveling effect where the different anionic complexes displayed similar oxidation potentials. In terms of reactivity, both $[(MeCN)Ni(CF_3)_3]^-$ and $[(MeCN)Ni(C_4F_8)(CF_3)]^-$ catalyze the trifluoromethylation of an electron rich arene with similar yields using Umemoto Reagent II as the electrophile. The cyclic voltammograms of the anionic derivatives can be significantly tuned by the replacement of the MeCN ligands with the NHC ligand IMes (1,3-bis(2,4,6-trimethylphenyl)imidazol-2-ylidene). The first oxidation potentials of $[(IMes)Ni(CF_3)_3]^-$ and $[(IMes)Ni(C_4F_8)(CF_3)]^-$ complexes were similar to that seen for $[(MeCN)Ni(CF_3)_3]^-$, but an oxidation wave occurring at more positive potentials was well-separated only for the NHC-containing derivatives. The same was observed for the $[(F\text{-}NHC)Ni(R_F)_3]^-$ complexes containing fluorinated phenyl substituents (*F*-NHC = 1,3-bis(2,4-F_2-Ph)-, 2,4,6-F_3-Ph- or 3,4,5-F_3-Ph)imidazol-2-ylidene; R_f = CF_3 or C_2F_5). This identification of a ligand environment that better separates oxidation potentials in the anionic Ni perfluoroalkyl complexes is expected to aid in the development of new (electro)catalytic methods that target single electron oxidations in order to release trifluoromethyl and perfluoroalkyl radicals.

Experimental section

General

All manipulations were performed using standard Schlenk and high vacuum techniques or in a N_2 filled glovebox, unless otherwise stated. Solvents were purified by passing through activated alumina and/or copper in a solvent purification system supplied by Pure Process Technology.

Instrumentation

^{19}F NMR spectra were recorded on the Bruker NMR spectrometer operating at 376 MHz and referenced to α,α,α-trifluorotoluene as an internal standard (δ = –63.7). 400 MHz ^{1}H NMR and 376 MHz ^{19}F NMR spectra of compounds **2**, **3**, **4**, and **6** were recorded on a Bruker 400 MHz spectrometer in CD_3CN. 400 MHz ^{1}H NMR spectra of **7**, **8**, and **9** were measured on a Bruker 400 MHz spectrometer in CD_3CN and 470.6 MHz ^{19}F NMR spectra of **7**, **8**, and **9** were measured on a Bruker 500 MHz spectrometer in CD_3CN. Cyclic voltammetry was measured using PARSTAT 4000A or a Metrohm μStat400 potentiostat on 10 mM solutions of the metal complexes containing 100 mM *n*-Bu_4NPF_6 electrolyte; using Pt or glassy carbon working and Pt counter electrodes, a Ag pseudo reference, at a scan rate of 100 mV/s. The ferrocene/ferrocenium (Fc/Fc^+) couple served as internal reference.

Single crystal X-ray diffraction

X-ray crystal structure determinations of **2**, **3**, **4**, and **6** were carried out on a Bruker D8 Quest diffractometer at 150(2) K using Mo-Kα radiation. Structure determinations of **7**, **8** and **9** were carried out on a Bruker D8 Venture using Mo-Kα radiation at 120 K. Structure solution and refinement details can be found in the ESI and cif-files.

Materials

IMes (1,3-bis(2,4,6-trimethylphenyl)-1,3-dihydro-2*H*-imidazol-2-ylidene) was obtained from Sigma-Aldrich and used without further purification. The starting Ni complex $[(MeCN)_2Ni(C_4F_8)]$ (**1**) was prepared as previously described.[29] 1,3-bis(2,4-difluorophenyl)imidazolium chloride and 1,3-bis(2,4,6-trifluorophenyl)imidazolium chloride were synthesized according to a literature procedure.[36]

Synthetic procedures

Preparation of 1,3-bis(3,4,5-trifluorophenyl)imidazolium chloride:

Under ambient conditions 3,4,5-trifluoroaniline (2.0 g, 13.6 mmol, 2.0 equiv.) was dissolved in 30 mL MeOH. Under stirring glyoxal (0.39 g, 6.8 mmol, 1.0 equiv.) was added as a 40 wt% aqueous solution. 3 drops of formic acid were added to the mixture and the solution was stirred for 7 d. The solution turned brown and colorless precipitate formed. The solids were filtered off, washed with cold MeOH and dried under reduced pressure. 1.16 g (3.67 mmol, 54%) colorless solid were isolated and immediately used for the following reaction without analysis. *N,N'*-bis(3,4,5-trifluorophenyl)-ethylenediimine (1.16 g, 3.67 mmol, 1.0 equiv.) was dissolved in 25 mL EtOAc. *p*-formaldehyde (0.11 g, 3.67 mmol, 1.0 equiv.) was added and the suspension was refluxed for 20 min. Trimethylchlorosilane (0.47 mL, 0.40 g, 3.67 mmol, 1.0 equiv.) was diluted in 10 mL EtOAc and added dropwise into the refluxing solution. After complete addition the mixture was refluxed another 2 h. The solid was filtered off, washed with EtOAc and diethyl ether and dried under reduced pressure. 0.53 g (1.45 mmol, 21% Yield) 1,3-bis(3,4,5-trifluorophenyl)imidazolium chloride were obtained as a colorless powder. ^{1}H NMR (DMSO-D_6, 500 MHz): δ = 10.75 (s, 1H), 8.62 (s, 2 H), 8.23 (t, *J* = 7.41 Hz, 4H). ^{19}F NMR (DMSO-D_6, 470.6 MHz): δ = –134.15 (dd, *J* = 21.8 Hz, *J* = 8.5 Hz, 4F), –160.65 (tt, *J* = 21.9 Hz, *J* = 5.0 Hz, 2F). HR-EI-MS (70 eV, 50-225°C, $C_{15}H_7N_2F_6Cl$): m/z = 344.03755 (–HF), 329.05061 (–Cl), 328.04250 (–HCl), 171.02890 ($C_8H_4F_3N$), 158.02109 ($C_7H_3F_3N$), 144.01806 (C_6HF_3N). Anal. Calcd (found) for $C_{15}H_7F_6N_2Cl$: C, 49.40 (47.40); H 1.93 (1.98); N 7.68 (7.70)%.

Preparation of $[NMe_4][(MeCN)(CF_3)Ni(C_4F_8)]$ (**2**): In a nitrogen filled glovebox, AgF (111 mg, 0.875 mmol, 1 equiv.) and TMS–CF_3 (0.20 mL, 1.31 mmol, 1.5 equiv.) were stirred in 10 mL of anhydrous MeCN for 2 h. A solution of $[(MeCN)_2Ni(C_4F_8)]$ (298 mg, 0.874 mmol, 1 equiv.) in 1 mL of anhydrous MeCN was added dropwise to the reaction mixture followed by addition of NMe_4Cl (91 mg, 0.874 mmol, 1 equiv.). The reaction was stirred for one day at room temperature and filtered through a pad of Celite. The resulting black-red solution was dried in vacuo to a dark brown paste. The paste was dissolved in a minimal amount of THF followed by the addition of pentane and cooling to –30 ^{0}C. The resulting black/brown solid was washed with pentane and dried under vacuum. Yield: 278 mg (72%). X-ray quality crystals were grown by cooling a saturated solution of THF. ^{1}H NMR (CD_3CN, 400 MHz): δ = 3.07 (s, 12H). ^{19}F NMR (CD_3CN, 376 MHz): δ = –31.4 (quintet, *J* = 3.5 Hz, 3F), –109.3 (app decet, *J* = 4.1 Hz, 2F), –117.3 (apparent octet, *J* = 3.6 Hz, 2F), –139.0 to –139.3 (m, 2F), –141.0 to –141.1 (m, 2F). Anal. Calcd. (found) for $C_{11}H_{15}NiF_{11}N_2$: C, 29.83 (29.60); H, 3.41 (3.69)%.

Preparation of [NMe$_4$][(MeCN)(CF$_3$CF$_2$)Ni(C$_4$F$_8$)] (**3**): In a nitrogen filled glovebox, AgF (106 mg, 0.835 mmol, 1.05 equiv.) and TMS–C_2F_5 (0.21 mL, 1.19 mmol, 1.5 equiv.) were stirred in 10 mL of anhydrous MeCN for 2 h. A solution of the [(MeCN)$_2$Ni(C$_4$F$_8$)] (271 mg, 0.795 mmol, 1 equiv.) in 1 mL of anhydrous MeCN was added dropwise to the reaction mixture followed by addition of NMe_4Cl (88 mg, 0.795 mmol, 1 equiv.). The reaction was stirred for 2 days at room temperature and filtered through a pad of Celite. The resulting brown solution was dried in vacuo. The paste was dissolved in a minimal amount of THF followed by the addition of pentane and cooling to –30^{0}C. The black/brown solid was washed with pentane and dried under vacuum. Yield: 293 mg (75%). ^{1}H NMR (CD_3CN, 400 MHz): δ = 3.07 (s, 12H) ^{19}F NMR (CD_3CN, 376 MHz): δ = −82.5 (t, *J* = 3.8 Hz, 3F), –110.2 (app tetradecet, *J* = 3.7 Hz, 2F), –112.1 (app t, *J* = 6.8 Hz, 2F), –116.6 (app sextet, *J* = 3.9 Hz, 2F), –139.2 to –139.4 (m, 2F), –140.9 to –141.1 (m, 2F). Anal. Calcd. (found) for $C_{12}H_{15}NiF_{13}N_2$: C, 29.24 (29.10); H, 3.07 (3.21)%.

Preparation of [NMe$_4$][(IMes)(CF$_3$)Ni(C$_4$F$_8$)] (**4**): In a nitrogen filled glovebox, to a stirring solution of [NMe$_4$][(MeCN)(CF$_3$)Ni(C$_4$F$_8$)] (81 mg, 0.18 mmol, 1 equiv.) in 0.5 mL of MeCN, a solution of IMes (69 mg, 0.23 mmol, 1.3 equiv.) in 1.5 mL of MeCN was added and stirred for 2 h. The reaction was filtered over a pad of Celite and the solvents were removed under vacuum. The resulting solid was collected and washed with ether to yield 88 mg of black solid (69%). ^{1}H NMR (CD_3CN, 400 MHz): δ = 7.11 (br s, 1H), 7.06 (br s, 2H), 7.00 (br s, 2H), 3.06 (br s, 12H), 2.37 – 2.33 (br m, 6H), 2.26 (br s, 6H), 2.17 (br s, 6H). ^{19}F NMR (CD_3CN, 376 MHz): δ = –23.2 (br s, 3F), –109.5 (s, 2F), –113.0 to –113.1 (m, 2F), –138.5 to –138.8 (m, 2F), –139.3 to –139.6 (m, 2F). Anal. Calcd. (found) for $C_{30}H_{36}NiF_{11}N_3$: C: 51.02 (53.55); H 5.14 (5.69)%. A better elemental analysis of this compound could not be obtained, likely due to co-crystallized solvent, as was found in the preliminary X-ray data set (see ESI).

Preparation of [NMe$_4$][(IMes)Ni(CF$_3$)$_3$] (**6**): In a glovebox, to a stirring solution of [NMe$_4$][(MeCN)Ni(CF$_3$)$_3$] (60 mg, 0.16 mmol, 1 equiv.) in 0.5 mL of MeCN, a solution of IMes (58 mg, 0.19 mmol, 1.2 equiv.) in 1.5 mL of MeCN was added and stirred for 4 h. The insoluble were removed, and the volatiles were removed under vacuum. The precipitate was collected and washed with ether to yield 68 mg (66%) of light yellow solid. ^{1}H NMR (CD_3CN, 376 MHz): δ = 7.05 (s, 2H), 7.03 (br s, 4H), 3.07 (br s, 12H), 2.36 (s, 6H), 2.28 (s, 12H). ^{19}F NMR (CD_3CN, 376 MHz): δ = –22.9 (q, *J* = 5.3 Hz, 6F), –26.8 (sept, *J* = 5.3 Hz, 3F). Anal. Calcd (found) for $C_{28}H_{36}NiF_9N_3$: C, 52.20 (52.07); H, 5.63 (5.55)%.

Preparation of [NMe$_4$][(2,4-F$_2$Ph)Ni(CF$_3$)$_3$] (**7**) / **[NMe$_4$][(2,4-F$_2$Ph)Ni(C$_2$F$_5$)(CF$_3$)$_2$]** (**7′**): In an inert *Schlenk*-tube 1,3-bis(2,4-difluorophenyl)imidazolium chloride (170 mg, 0.52 mmol, 1 equiv.) was suspended in 5 mL THF. The suspension was cooled to 0 °C. 1.02 mL KHMDS solution (0.5 M in toluene) were added to the NHC·HCl salt. The mixture was stirred until the suspended NHC·HCl salt had dissolved. [NMe$_4$][(MeCN)Ni(CF$_3$)$_3$] (197 mg, 0.52 mmol, 1 equiv.) was suspended in 5 mL THF and added *via* cannula. The mixture was stirred for 15 min at 0°C and then brought to room temperature. The insolubles were removed and the orange solution was layered with *n*-pentane. The layered solutions were stored in a box freezer at -18 °C until the solutions had fully mixed, precipitating a 3.5:1 mixture of NMe$_4$[Ni(CF$_3$)$_3$(1,3-bis(2,4-difluorophenyl)imidazol-2-ylidene)]) and NMe$_4$[Ni(C$_2$F$_5$)(CF$_3$)$_2$(1,3-bis(2,4-difluorophenyl)imidazol-2-ylidene)]). The solution was decanted and the solids were dried under reduced pressure, yielding 155 mg product mixture which could not be separated. ^{1}H NMR (CD_3CN, 400 MHz): δ = 8.73-8.82 (m, 0.6H), 8.61-8.71 (m, 2H), 7.37-7.40 (m, 2.4H), 7.23-7.30 (m, 2.8H), 7.15-7.23 (m, 2.8H), 3.13 (s, 26H). ^{19}F NMR (CD_3CN, 470.6 MHz, NMe$_4$[Ni(CF$_3$)$_3$(1,3-bis(2,4-difluorophenyl)imidazol-2-ylidene)]): δ = -23.89 (br q, *J* = 4.4 Hz, 6F), –27.45 (sept, *J* = 4.4 Hz, 3F), –111.64 (quintet, *J* = 6.6 Hz, 2F, F-4), –120.58 (br q, *J* = 8.2 Hz, 2F; F-2). ^{19}F NMR (CD_3CN, 470.6 MHz, NMe$_4$[Ni(C$_2$F$_5$)(CF$_3$)$_2$(1,3-bis(2,4-

difluorophenyl)imidazol-2-ylidene)]): δ = –23.30 (br s, 3F), –26.70 (sept, J = 5.9 Hz, 3F), –81.73 (q, J = 6.1 Hz, 3F), –98.96 (br s, 2F), –111.92 (quintet, J = 7.0 Hz, 2F, F-4), –120.32 (br q, J = 7.6 Hz), 2F, F-2).

Preparation of $[NMe_4][(2,4,6\text{-}F_3Ph)Ni(CF_3)_3]$ (8) / $[NMe_4][(2,4,6\text{-}F_3Ph)Ni(C_2F_5)(CF_3)_2]$ (8′): In an inert *Schlenk*-tube 1,3-bis(2,4,6-trifluorophenyl)imidazolium chloride (154 mg, 0.42 mmol, 1 equiv.) was suspended in 5 mL THF. The suspension was cooled to 0 °C. 0.84 mL KHMDS solution (0.5 M in toluene) were added to the NHC·HCl salt. The mixture was stirred until the suspended NHC·HCl salt had dissolved. $[NMe_4][(MeCN)Ni(CF_3)_3]$ (161 mg, 0.42 mmol, 1 equiv.) was suspended in 5 mL THF and added *via* cannula. The mixture was stirred for 15 min at 0 °C and then brought to room temperature. The insolubles were removed and the orange solution was layered with *n*-pentane. The layered solutions were stored in a box freezer at -18 °C until the solutions had fully mixed, precipitating a 1.7:1 mixture of $NMe_4[Ni(CF_3)_3$(1,3-bis(2,4,6-trifluorophenyl)imidazol-2-ylidene)]) and $NMe_4[Ni(C_2F_5)(CF_3)_2$(1,3-bis(2,4,6-trifluorophenyl)imidazol-2-ylidene)]). The solution was decanted and the solids were dried under reduced pressure, yielding 176 mg product mixture which could not be separated. ^1H NMR (CD_3CN, 400 MHz): δ = 7.30 (s, 2H), 7.27 (s, 1H), 7.05-7.16 (m, 6H), 3.09 (s, 19H). ^{19}F NMR (CD_3CN, 470.6 MHz, $NMe_4[Ni(CF_3)_3$(1,3-bis(2,4,6-trifluorophenyl)imidazol-2-ylidene)]): δ = -25.16 (sextett, J = 4.4 Hz, 6F), -28.18 (sept, 4.6 Hz, 3F), -108.59 to -108.72 (m, 2F, F-4), -114.03 (br s, 4F, F-2,6). ^{19}F NMR (CD_3CN, 470.6 MHz, $NMe_4[Ni(C_2F_5)(CF_3)_2$(1,3-bis(2,4,6-trifluorophenyl)imidazol-2-ylidene)]): δ = –24.33 (br s, 3F), –26.55 (br s, 3F), –80.02 (br q, J = 8.3 Hz, 3F), –98.22 (br s, 2F), –108.74 to -108.85 (m, 2F, F-4), -113.69 (br s, 4F, F-2,6).

Preparation of $[NMe_4][(3,4,5\text{-}F_3Ph)Ni(CF_3)_3]$ (9) / $[NMe_4][(3,4,5\text{-}F_3Ph)Ni(C_2F_5)(CF_3)_2]$ (9′): In an inert *Schlenk*-tube 1,3-bis(3,4,5-trifluorophenyl)imidazolium chloride (76 mg, 0.26 mmol, 1 equiv.) was suspended in 5 mL THF. The suspension was cooled to 0°C. 0.52 mL KHMDS solution (0.5 M in toluene) were added to the NHC·HCl salt. The mixture was stirred until the suspended NHC·HCl salt had dissolved. $[NMe_4][(MeCN)Ni(CF_3)_3]$ (79 mg, 0.26 mmol, 1 equiv.) was suspended in 5 mL THF and added *via* cannula. The mixture was stirred for 15 min at 0 °C and then brought to room temperature. The insolubles were removed and the orange solution was layered with *n*-pentane. The layered solutions were stored in a box freezer at -18°C until the solutions had fully mixed, precipitating a 1.8:1 mixture of $NMe_4[Ni(CF_3)_3$(1,3-bis(3,4,5-trifluorophenyl)imidazol-2-ylidene)]) and $NMe_4[Ni(C_2F_5)(CF_3)_2$(1,3-bis(3,4,5-trifluorophenyl)imidazol-2-ylidene)]). The solution was decanted and the solids were dried under reduced pressure, yielding 41 mg product mixture which could not be separated. ^1H NMR (CD_3CN, 400 MHz): δ = 8.53-8.67 (m, 2H), 8.38-8.52 (m, 4H), 7.60 (s, 1H), 7.56 (s, 2H), 3.06 (s, 20H). ^{19}F NMR (CD_3CN, 470.6 MHz, $NMe_4[Ni(CF_3)_3$(1,3-bis(2,4,6-trifluorophenyl)imidazol-2-ylidene)]): δ = -23.79 (q, J = 4.2 Hz, 6F), –27.08 (sept, J = 4.0 Hz, 3F), –135.50 to –135.65 (m, 4F, F-3,5), –163.94 to -164.10 (tt, J = 20.4, J = 6.2, 2F, F-4). ^{19}F NMR (CD_3CN, 470.6 MHz, $NMe_4[Ni(C_2F_5)(CF_3)_2$(1,3-bis(3,4,5-trifluorophenyl)imidazol-2-ylidene)]): δ = -23.56 (br s, 3F), -26.56 (br s, 3F), -82.58 (q, J = 4.5 Hz, 3F), -99.91 to –100.00 (m, 2F), -135.67 to -135.80 (m, 4F, F-3,5), -164.28 to -164.43 (tt, J = 20.4, J = 6.2, 2F, F-4).

Catalytic trifluoromethylation of 1,3,5-trimethoxybenzene

In a nitrogen filled glovebox, a vial was charged with 1,3,5-trimethoxybenzene (42 mg, 0.25 mmol, 5 equiv.), Umemoto Reagent II (22 mg, 0.05 mmol, 1 equiv.), and 0.9 mL of DMSO. While stirring, 100 µL of a 0.025 M stock solution of $[NMe_4][(MeCN)(CF_3)Ni(C_4F_8)]$ in DMSO was added, and the reaction was continued to stir for 24 h. Trifluorotoluene (6.14 µL, 0.05 mmol, 1 equiv.) was added as an internal standard and the ^{19}F NMR was recorded. The NMR yield of the trifluoromethylated arene was determined to be 83%.

Electronic Supplementary Information (ESI) Available: Crystallographic information files (CIF) and selected NMR spectral data. This material is available free of charge via the internet at Accession Codes CCDC 2124819, 2124820, 2124821, 2095551, 2103215, 2118416, and 2133045 contain the supplementary crystallographic data for compounds **2**, **3**, **6**, **6′**, **7/7′**, **9**, and **9′** respectively. The binuclear $[Ni(CF_3)_4(\mu\text{-}F)_2]$

is deposited as 2126925. These data can be obtained free of charge via www.ccdc.cam.ac.uk/data_request/cif, by e-mailing to data_request@ccdc.cam.ac.uk, or by contacting The Cambridge Crystallographic Data Centre, 12 Union Road, Cambridge CB2 1EZ, UK; fax: +44 1223 336033.

Author contributions
All authors have read and agreed to the submitted version of the manuscript.

Conflict of interest
The authors declare no competing financial interests

Acknowledgements
D.A.V. thanks the Office of Basic Energy Sciences of the U. S. Department of Energy (DE-SC0009363) for support of this work. The authors thank Teng Xue for generously preparing the $[(MeCN)_2Zn((CF_2)_4)_2Zn(MeCN)_2]$ reagent used to prepare compound **1**. A.K. and S.S. thank the University of Cologne for support.

References

1. D. Y. Mikhaylov, Y. H. Budnikova, T. V. Gryaznova, D. V. Krivolapov, I. A. Litvinov, D. A. Vicic and O. G. Sinyashin, *J. Organomet. Chem.*, 2009, **694**, 3840–3843.
2. E. A. Meucci, S. N. Nguyen, N. M. Camasso, E. Chong, A. Ariafard, A. J. Canty and M. S. Sanford, *J. Am. Chem. Soc.*, 2019, **141**, 12872–12879.
3. Y. Wu, H.-R. Zhang, R.-X. Jin, Q. Lan and X.-S. Wang, *Adv. Synth. Catal.*, 2016, **358**, 3528–3533.
4. S. Zhang, F. Weniger, F. Ye, J. Rabeah, S. Ellinger, F. Zaragoza, C. Taeschler, H. Neumann, A. Brueckner and M. Beller, *Chem. Commun.*, 2020, **56**, 15157–15160.
5. C. Xu, Z.-F. Yang, L. An and X. Zhang, *ACS Catal.*, 2019, 9, 8224–8229.
6. C. Xu, R. Cheng, Y.-C. Luo, M.-K. Wang and X. Zhang, *Angew. Chem. Int. Ed.*, 2020, **59**, 18741–18747.
7. M. Zhou, H.-Y. Zhao, S. Zhang, Y. Zhang and X. Zhang, *J. Am. Chem. Soc.*, 2020, **142**, 18191–18199.
8. Y.-L. Xiao, W.-H. Guo, G.-Z. He, Q. Pan and X. Zhang, *Angew. Chem. Int. Ed.*, 2014, **53**, 9909–9913.
9. L. An, C. Xu and X. Zhang, *Nat. Commun.*, 2017, **8**, 1460 (1–9).
10. X. He, X. Gao and X. Zhang, *Chin. J. Chem.*, 2018, **36**, 1059–1062.
11. H.-Y. Zhao, X. Gao, S. Zhang and X. Zhang, *Org. Lett.*, 2019, **21**, 1031–1036.
12. X.-P. Fu, Y.-L. Xiao and X. Zhang, *Chin. J. Chem.*, 2018, **36**, 143–146.
13. C. Xu, W.-H. Guo, X. He, Y.-L. Guo, X.-Y. Zhang and X. Zhang, *Nat. Commun.*, 2018, **9**, 1–10.
14. H. X. Z. X. Gao Xing, *Chin. J. Org. Chem.*, 2019, **39**, 215–222.
15. W.-Q. Hu, S. Pan, X.-H. Xu, D. A. Vicic and F.-L. Qing, *Angew. Chem. Int. Ed.*, 2020, **59**, 16076–16082.
16. S. T. Shreiber, I. M. DiMucci, M. N. Khrizanforov, C. J. Titus, D. Nordlund, Y. Dudkina, R. E. Cramer, Y. Budnikova, K. M. Lancaster and D. A. Vicic, *Inorg. Chem.*, 2020, **59**, 9143–9151.
17. D. M. Ferguson, J. R. Bour, A. J. Canty, J. W. Kampf and M. S. Sanford, *Organometallics*, 2019, **38**, 519–526.
18. J. R. Bour, N. M. Camasso and M. S. Sanford, *J. Am. Chem. Soc.*, 2015, **137**, 8034–8037.

19. J. R. Bour, N. M. Camasso, E. A. Meucci, J. W. Kampf, A. J. Canty and M. S. Sanford, *J. Am. Chem. Soc.*, 2016, 138, 16105–16111.
20. J. Jover, F. M. Miloserdov, J. Benet-Buchholz, V. V. Grushin and F. Maseras, *Organometallics*, 2014, **33**, 6531-6543.
21. S. T. Shreiber and D. A. Vicic, *Angew. Chem. Int. Ed.*, 2021, **60**, 18162–18167.
22. M. D. Kosobokov, A. Sandleben, N. Vogt, A. Klein and D. A. Vicic, *Organometallics*, 2018, **37**, 521–525.
23. S. Yu, Y. Dudkina, H. Wang, K. V. Kholin, M. K. Kadirov, Y. H. Budnikova and D. A. Vicic, *Dalton Trans.*, 2015, **44**, 19443–19446.
24. J. R. Bour, D. M. Ferguson, E. J. McClain, J. W. Kampf and M. S. Sanford, *J. Am. Chem. Soc.*, 2019, **141**, 8914–8920.
25. G. M. Lee, I. Korobkov and R. T. Baker, *J. Organomet. Chem.*, 2017, **847**, 270–277.
26. T. Xue and D. A. Vicic, *Organometallics*, 2020, **39**, 3715–3720.
27. R. R. Burch, J. C. Calabrese and S. D. Ittel, *Organometallics*, 1988, **7**, 1642–1648.
28. N. O. Andrella, A. J. Sicard, S. I. Gorelsky, I. Korobkov and R. T. Baker, *Chem. Sci.*, 2015, **6**, 6392–6397.
29. P. T. Kaplan, L. Xu, B. Chen, K. R. McGarry, S. Yu, H. Wang and D. A. Vicic, *Organometallics*, 2013, 32, 7552–7558.
30. D. M. Wiemers and D. J. Burton, *J. Am. Chem. Soc*. 1986, **108**, 832–834.
31. M. M. Kremlev, W. Tyrra, A. I. Mushta, D. Naumann and Y. L. Yagupolskii. *J. Fluorine Chem.* 2010**, 131**, 212–216.
32. Q. Xie, L. Li, Z. Zhu, R. Zhang, C. Ni and J. Hu, *Angew. Chem. Int. Ed.* 2018, **57**, 13211–13215.
33. Y. Yamaguchi, H. Ichioka, A. Klein, W. W. Brennessel and D. A. Vicic, *Organometallics*, 2012, **31**, 1477–1483.
34. C.-P. Zhang, H. Wang, A. Klein, C. Biewer, K. Stirnat, Y. Yamaguchi, L. Xu, V. Gomez-Benitez and D. A. Vicic, *J. Am. Chem. Soc.*, 2013, **135**, 8141–8144.
35. N. G. Connelly and W. E. Geiger, *Chem. Rev.*, 1996, **96**, 877–910.
36. D. A. J. Harding, E. G. Hope, K. Singh and G. A. Solan, *Organometallics* 2012, **31**, 1518–1523.